

Field measurements from contrasting reefs show spurs and grooves can dissipate more wave energy than the reef crest

Stephanie Jane Duce¹, Ana Vila-Concejo², Robert Jak McCarroll³, Bevan Yiu⁴, Lachlan A Perris², and Jody M Webster²

¹James Cook University

²University of Sydney

³Department Environment, Land, Water and Planning. Victoria

⁴Sydney Water

November 21, 2022

Abstract

Coral reefs are widely recognized as effective dissipaters of wave energy. Spurs and grooves (SAG) are common features of fore reefs worldwide and are thought to be particularly efficient at dissipating wave energy. However, very few studies have collected in-situ hydrodynamic data to verify this and understand SAG interactions with hydrodynamic forces. We present in-situ wave data from contrasting SAG sites at Moorea, French Polynesia and One Tree Reef in the southern Great Barrier Reef, Australia. We measured extremely high rates of wave energy dissipation (up to 0.1 kW/m) than the adjacent spur (mean = 0.01 kW/m²). Correlations between measured dissipation, wave height and depth allowed us to develop a conceptual model showing that SAGs dissipate more energy under high wave conditions at low tides, while the reef crest dissipates more energy at high tides under small wave conditions. Further study is required to better understand and model the hydrodynamics of SAG zones and the important role they play in reef dynamics and coastal protection.

1 Field measurements from contrasting reefs show spurs and grooves can
2 dissipate more wave energy than the reef crest
3

4 **S. Duce^{1,2}, A. Vila-Concejo², R. J. McCarroll^{2,3}, B. Yiu⁴, L. A. Perris², and J. M.**
5 **Webster²**

6
7 ¹TROPwater, College of Science and Engineering, James Cook University, Bebegu Yumba
8 Campus, Townsville, Queensland, 4811, Australia
9

10 ²Geocoastal Research Group, School of Geosciences, University of Sydney, Sydney, New
11 South Wales, 2006, Australia.
12

13 ³Department Environment, Land, Water and Planning, East Melbourne, Victoria, Australia
14

15 ⁴Field Sampling & Testing, Sydney Water, 51 Hermitage Road, West Ryde, NSW, 2114,
16 Australia
17

18 Corresponding author: Stephanie Duce (stephanie.duce@jcu.edu.au)
19

20 **Key Points:**

- 21 • Field measurements show extremely high wave energy dissipation rates (up to 0.1
22 kW/m²) across the SAG zone due to bottom friction alone.
23
- 24 • SAGs were more effective at dissipating wave energy than the reef crest across
25 differing reef morphologies and hydrodynamic regimes.
26
- 27 • Greater dissipation at sites with high coral cover and mesotidal range suggest live
28 coral and tidal currents contribute to dissipation.
29

30

31

32

33

34

35 **Abstract**

36 Coral reefs are widely recognized as effective dissipaters of wave energy. Spurs and grooves
37 (SAG) are common features of fore reefs worldwide and are thought to be particularly
38 efficient at dissipating wave energy. However, very few studies have collected in-situ
39 hydrodynamic data to verify this and understand SAG interactions with hydrodynamic forces.
40 We present in-situ wave data from contrasting SAG sites at Moorea, French Polynesia and
41 One Tree Reef in the southern Great Barrier Reef, Australia. We measured extremely high
42 rates of wave energy dissipation (up to 0.1 kW/m^2) across the SAG zone due to bottom
43 friction alone. Interestingly, SAGs dissipated wave energy at higher rates than the reef crest
44 under the modal conditions measured. Rates of dissipation were the greatest at sites with high
45 live coral cover in mesotidal environments (i.e., One Tree Reef), suggesting the structural
46 complexity of live corals increases bed friction and that tidal currents may contribute to
47 dissipation. Unexpectedly, rates of dissipation were higher across the groove (mean $\epsilon=0.04$
48 kW/m^2) than the adjacent spur (mean $\epsilon=0.01 \text{ kW/m}^2$). Correlations between measured
49 dissipation, wave height and depth allowed us to develop a conceptual model showing that
50 SAGs dissipate more energy under high wave conditions at low tides, while the reef crest
51 dissipates more energy at high tides under small wave conditions. Further study is required to
52 better understand and model the hydrodynamics of SAG zones and the important role they
53 play in reef dynamics and coastal protection.

54

55 **Plain Language Summary**

56 Coral reefs play an essential role in reducing the impact of waves on adjacent coastal areas
57 and infrastructure. However, due to the difficulty of working in high energy wave
58 environments, little is known about how different reef zones dissipate wave energy. To
59 address this research gap, we used pressure sensors to measure the height and power of waves
60 across different coral reef zones at One Tree Reef in the Great Barrier Reef, Australia, and
61 Moorea in French Polynesia. We examined how waves dissipate their energy as they move
62 across the reef from the fore reef, a deeper zone characterised by finger-like coral structures
63 called spurs and grooves, to the reef crest, a shallower area where waves often break, and
64 which is assumed to be responsible for most wave energy dissipation. Surprisingly, we found
65 that the fore reef spur and groove zone was often more effective in dissipating wave energy
66 than the reef crest. Tidal stage and wave height were important in determining how much the

67 waves interact with the seafloor and loose energy due to friction. Our study also found initial
68 evidence that the amount of live coral cover is important, with higher dissipation found in
69 areas with higher live coral cover. Further field studies measuring wave dissipation across
70 reef zones will help us better understand and model this system and its importance in coastal
71 protection.

72

73 **1. Introduction**

74 Waves are the main hydrodynamic force acting on coral reefs and are a crucial driving
75 factor in the formation, growth and persistence of coral reefs across all spatial and temporal
76 scales (Harris et al., 2015; Storlazzi et al., 2005). Reef hydrodynamics control the transport
77 and deposition of spawn, larvae and recruits, the provision of nutrients, removal of wastes
78 and the production and transport of biogenic sediments to form the reef and associated
79 features such as reef islands (Masselink et al., 2020). Coral reefs have long been recognized
80 as providing effective wave energy dissipation and protecting coastlines (e.g. Munk &
81 Sargent, 1948). The value of reefs as natural breakwater systems has become particularly
82 important with growing threats from rising sea levels and increased storm activity (e.g. Beck
83 et al., 2018; Ferrario et al., 2014; Foley et al., 2014; Gallop et al., 2014; Van Zanten et al.,
84 2014; Vila-Concejo et al., 2017; Woodhead et al., 2019).

85 Numerical modelling of wave dissipation across coral reefs has become a relatively
86 common tool to inform coastal management and predict the likely effects of sea level rise
87 (Baldock et al., 2019; Baldock et al., 2020; Bramante et al., 2020; Harris et al., 2018).
88 Accurate and high-resolution field data are required to calibrate and validate numerical
89 models and optimize their utility (e.g. Horstman et al., 2014; Storlazzi et al., 2011). However,
90 the remote location of many coral reefs makes access difficult, and it is challenging to deploy
91 instruments particularly in the high-energy fore reef zone. Nevertheless, field observations in
92 fore reef environments are necessary to examine dissipation under complex natural
93 conditions and to understand sediment production and transport in biogenic coral reef
94 systems.

95 The majority of existing studies detailing wave dissipation by coral reefs measure
96 dissipation across reef flats (e.g. Brander et al., 2004; Hardy & Young, 1996; Harris & Vila-
97 Concejo, 2013; Harris et al., 2015; Huang et al., 2012; Kench & Brander, 2006) and around
98 reef islands (e.g. Beetham & Kench, 2014; Kench et al., 2009; Mandlier, 2013; Samosorn &

99 Woodroffe, 2008). Given the logistical complexity of instrument deployments on reefs, some
100 studies have measured wave dissipation across the reef crest based on a single instrument on
101 the fore reef and another on the reef flat behind the reef crest (e.g. Lowe, 2005; Lugo-
102 Fernández et al., 1998a; Lugo-Fernández et al., 1998b; Pomeroy et al., 2012; Cheriton et al.,
103 2016). These studies provide robust evidence of coral reefs' ability to dissipate wave energy
104 but do not provide spatial resolution to differentiate wave dissipation occurring on the fore
105 reef from that of the reef crest and reef flat. Notable exceptions are Monismith et al. (2015),
106 Monismith et al. (2013), Péquignet et al. (2011) and Storlazzi et al. (2004), where wave
107 measurements included at least two fore reef locations. On the fore reef of Palmyra Atoll,
108 Monismith et al. (2015) calculated the highest friction factor (1.8) measured at any reef, with
109 approximately 20% wave energy dissipation over 56 m (i.e., 35.7% over 100 m) and
110 suggested that healthy coral cover facilitated efficient wave dissipation.

111 Spurs and grooves (SAG) are a common geomorphic feature of many fore reefs
112 worldwide and their origin and formation mechanisms have been the subject of some debate
113 (Gischler, 2010). They are characterized by parallel ridges of carbonate material (spurs),
114 separated by channels (grooves) which are usually aligned perpendicular to the reef front.
115 The features show considerable variations in morphology which are thought to be
116 predominantly driven by the prevailing hydrodynamic energy (Duce et al., 2020; Duce et al.,
117 2016; Roberts, 1974; Storlazzi et al., 2003). However, very few studies have collected in-situ
118 hydrodynamic data to verify this, let alone attempt to understand the mechanics and spatial
119 variability of wave energy dissipation by the SAG.

120 To date wave hydrodynamics across SAGs have only been directly measured at three
121 reefs worldwide; Grand Cayman Island in the Caribbean (Roberts et al., 1975), Molokai,
122 Hawaii (Storlazzi et al., 2004) and Ipan, Guam (Péquignet et al., 2011) in the central Pacific.
123 At Grand Cayman, Roberts et al. (1975) found that bottom friction at the fore reef SAGs
124 modified deep water waves and currents reducing wave heights by ~20% (i.e., 0.5% per 10
125 m) and current speeds by ~60-70% over the ~400 m between the outer instrument (21 m
126 depth) and inner instrument (8 m depth). Storlazzi et al. (2004) measured less than 0.1%
127 dissipation in wave power per 10 m for small waves ($H_s < 0.4$ m) across the SAG zone at
128 Molokai, Hawaii. Péquignet et al. (2011) measured a 17% decline in wave energy flux during
129 a tropical cyclone over 55 m (i.e., 3.1% per 10 m) between sensors at 7.9 and 5.7 m depth on
130 the fore reef SAGs at Ipan fringing reef in Guam and found that the majority of energy was
131 dissipated by wave breaking in the surf zone.

132 In this paper, we quantify the wave energy dissipation across different types of SAG in
133 two contrasting coral reef types and determine the mechanisms by which most dissipation
134 occurs at each site (i.e., wave breaking at the reef crest versus bottom friction across the fore
135 reef). Further, we assess the influence of other variables including offshore wave height,
136 water depth, spur and groove morphology, tidal currents and coral cover on energy
137 dissipation. This paper also presents comprehensive wave datasets, including measurements
138 at the inner and outer limits of the SAG zone at five sites located on two contrasting reefs
139 under different tidal and wave energy regimes. These sites are Moorea in French Polynesia
140 and One Tree Reef in the southern Great Barrier Reef (GBR).

141

142 **2. Study Sites**

143 We undertook 10 field experiments, five at One Tree Reef in the southern GBR,
144 Australia and five at Moorea, French Polynesia. The field experiments included areas from
145 each reef with different degrees of wave exposure (Figures 1 and 2) with wave measurements
146 undertaken across the SAG zone of the fore reef. Each site is described in detail in
147 Supplementary Text S1-S5.

148 **2.1 Moorea**

149 Moorea (17°30' S, 149°50' W) is a high volcanic island in French Polynesia, in the
150 central tropical South Pacific Ocean (Figure 1). The island has a perimeter of 60 km and is
151 surrounded by a barrier reef between 0.5 to 1 km from shore protecting an inshore lagoon
152 (Leichter et al., 2012). Several passes around the reef connect the inshore lagoons with the
153 open ocean (Figure 1b). Between 1 and 2 km offshore of the reef, water depths drop to > 500
154 m (Leichter et al., 2013). Moorea is micro-tidal with a spring tidal range of 0.2 m (Hench et
155 al., 2008). It is exposed to seasonal oceanic swells with significant wave heights between 1
156 and 2 m, however significant wave heights between 5 to 8 m, associated with storms and
157 remotely generated swell, are not uncommon (Leichter et al., 2013). The dominant swell
158 direction is from the southwest. From approximately October to April, the northern shore of
159 Moorea receives northerly swells driven by storms across the Northern Pacific (Hench et al.,
160 2008). Waves are the dominant driver of currents over the reef crest as tides and wind-driven
161 flows are relatively weak (Hench et al., 2008; Monismith et al., 2013).

162 Since quantitative scientific studies began in the 1970s, Moorea reef has experienced
163 a number of stressors in the form of recurrent bleaching events (Adjeroud et al., 2009), two
164 major outbreaks of Crown-of-Thorns sea stars (Traçon et al., 2011) and cyclones, particularly

165 Cyclone Oli in 2010 (Etienne, 2012). These events caused coral cover on the fore reef to
166 decline from > 40% in 2005 to < 5% in 2010 (Kayal et al., 2012). By 2013 Scleractinian coral
167 cover at Moorea fore reef (10 m depth) had recovered to approximately 20% and was
168 composed almost entirely of juveniles (Edmunds & Leichter, 2016). SAGs are visible in
169 satellite imagery around the entire fore reef of the barrier system.

170

171 **2.2 One Tree Reef**

172 One Tree Reef (OTR, 23°30' S, 152°05' E) is a lagoonal (mature) reef in the Capricorn-
173 Bunker Group of reefs in the southern GBR (Hopley et al., 2007). The reef lies within a
174 “Scientific Zone” of the GBR Marine Park, 80 km seaward of mainland Australia and hence
175 has minimal anthropogenic influences. It is located only 20 km west of the edge of the
176 continental shelf and is therefore exposed to the southeast trade winds and modal swell
177 energy for most of the year (Frith and Mason, 1986). The average annual significant wave
178 height is approximately 1.15 m from a predominantly east southeasterly direction driven by
179 trade winds (Hopley et al., 2007) and occasional cyclones also occur (e.g. Woolsey et al.,
180 2012). The reef is mesotidal and has semidiurnal tides with a mean spring tidal range of 3 m
181 (Vila-Concejo et al., 2014). The reef crest is mostly unbroken with no clear passes, and the
182 lagoon is isolated from swell and tides during approximately five hours of each tidal cycle
183 (Frith & Mason, 1986). There are high levels of live coral cover, particularly on the fore reef,
184 and a diverse range of calcifiers are present (Hamylton et al., 2013). SAGs are present around
185 the entire fore reef with four distinct classes associated with the different levels of wave
186 energy and antecedent topography (Duce et al., 2016). Duce et al. (2020) demonstrated that
187 the formation and evolution of SAGs at OTR could include growth offshore or onshore
188 depending primarily on wave exposure. The presence of a rubble cay on the southwest corner
189 of the reef flat and several active rubble spits along the reef flats demonstrate sediment
190 transport from the fore reef (Bryson et al., 2016; Shannon et al., 2013).

191

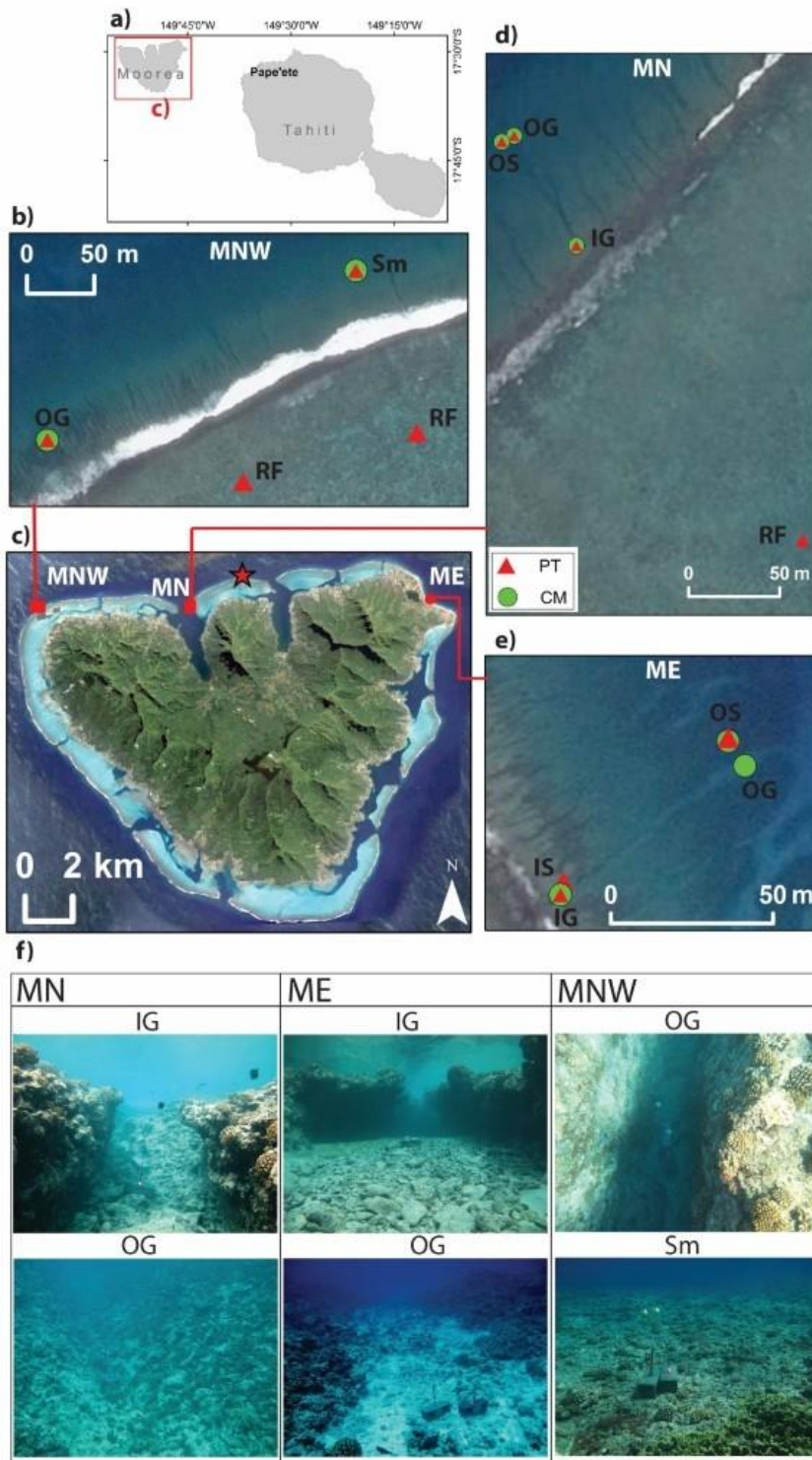


Figure 1 The location of Moorea adjacent to Tahiti in the South Pacific Ocean (a). Panel (c) shows an overview of the island where the star represents the location of the FOR01 wave mooring. Imagery of the study sites Moorea Northwest (MNW) (b); Moorea North (MN) (d) and Moorea East (ME) (e) are presented. The position of pressure sensors (PS - triangles) and current meters (CM – circles, Note: current meter data is not presented in this paper) are shown and labelled IG (inner groove), OG (outer groove), OS (outer spur), IS (inner spur), SFR (smooth fore reef) and RF (reef flat). Photographs of the deployment sites are shown in (f).

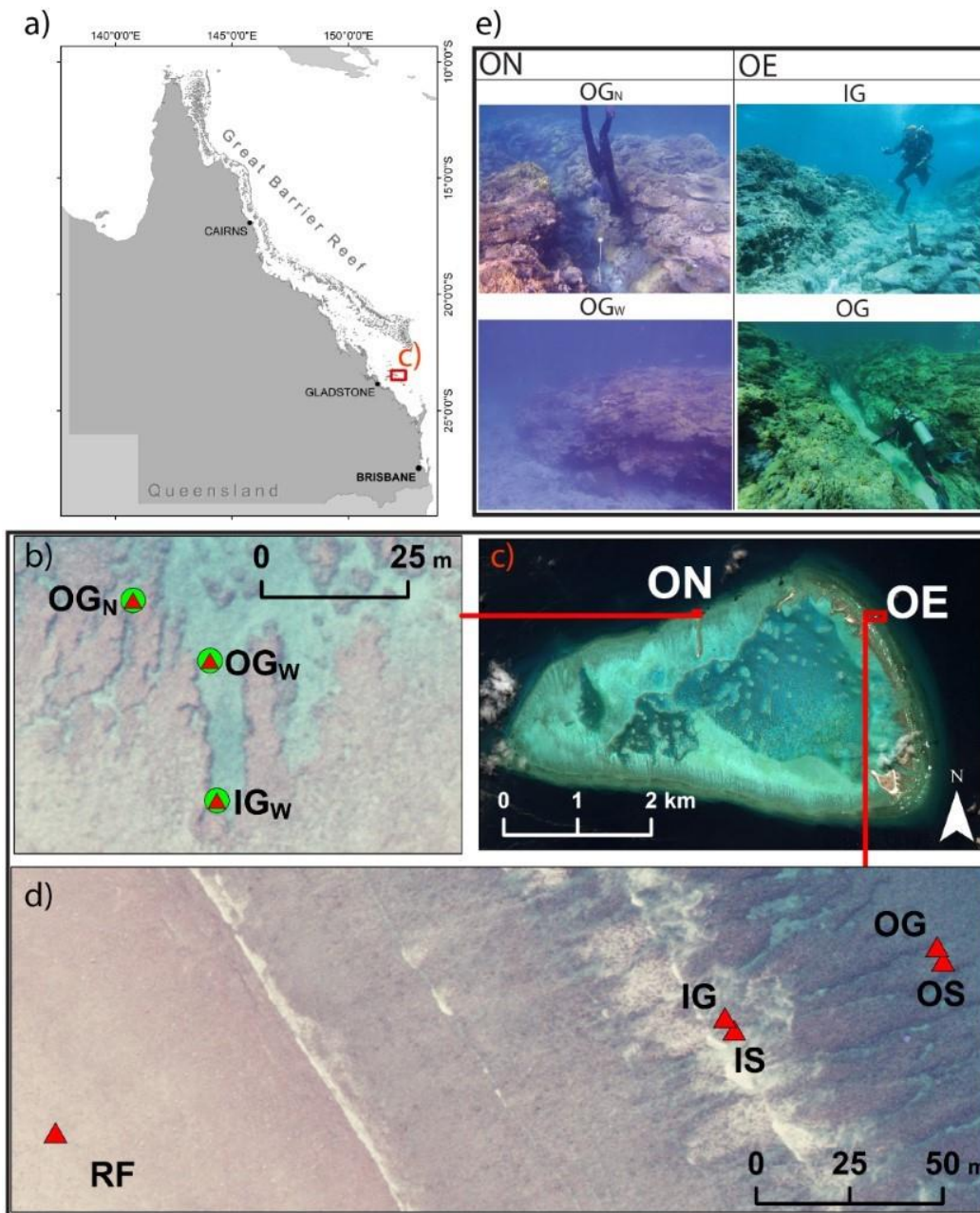


Figure 2 Overview of the location of One Tree Reef in the southern Great Barrier Reef (a) and the position of study sites around the reef (c). The position of pressure sensors (PS - triangles) and current meters (CM – circles). Note: current meter data is not presented in this paper) at One Tree north (ON) (b) and One Tree east (OE) (d) are shown and labelled IG (inner groove), OG (outer groove), OS (outer spur), IS (inner spur) and RF (reef flat). At ON (b) subscript _N denotes narrow groove and _w denotes wide groove. Photographs of the deployment sites are presented in (e).

193

194 3. Methods

195 3.1 Offshore wave data

196 Offshore wave data during our deployments at Moorea were obtained from the Moorea
 197 Coral Reef Long-Term Ecological Research (MCR LTER) mooring FOR01 on the northern
 198 fore reef (17.475°S, 149.837°E, Figure 1c) at a depth of approximately 10 m (Washburn,

199 2015) and from the WaveWatch III (WW3) global hindcast wave model (Tolman, 2009).
200 Wind data were obtained from Gump Station (Washburn & Brooks, 2016). Offshore wave
201 data at One Tree Reef were obtained from a Nortek Acoustic Waves and Currents Sensor
202 (AWAC) deployed at the One Tree East Mooring (23° 28.999' S, 152° 10.356' E) at a depth
203 of 15 m on the continental shelf 8 km east of One Tree Reef. Wind data were obtained from
204 the Australian Institute of Marine Science Integrated Marine Observing Station (AIMS
205 IMOS) weather station in the One Tree lagoon.

206

207 **3.2 Data collection**

208 The SAG zone, particularly the shallow area adjoining the reef crest, is extremely
209 dynamic and difficult to deploy instruments in, which explains the paucity of data collected
210 in this area to date. We deployed Aquistar INW PT2X pressure sensors at all sites, sampling
211 continuously at 4 Hz to measure wave characteristics. The length of the deployments was
212 typically short (<24 h) due to limited data storage in the instruments. The instruments were
213 cable tied to purpose-built concrete blocks with protruding metal rods that were placed by
214 SCUBA divers using lift bags. As shown by Duce et al. (2016) and Duce et al. (2020), the
215 same reef can support different SAG types thus deployments were conducted at multiple sites
216 on each reef to capture differing wave exposure regimes. Deployment locations included
217 three sites on the fore reef at Moorea – Moorea North West (MNW), Moorea North (MN)
218 and Moorea East (ME) (Figure 1); and two sites at One Tree Reef – One Tree East (OE) and
219 One Tree North (ON) (Figure 2). Detailed descriptions of each of these sites and the
220 instrument deployment configuration are available in Table 1 and the supplementary
221 materials (Supp. 1).

222 **Table 1** Overview of the deployments at Moorea and One Tree reefs including the geomorphic characteristics of the site and the dates of each
 223 deployment. For further information on each site refer to S1-S5. (The following acronyms are used in this table: MN: Moorea North; ME:
 224 Moorea East; MNW: Moorea North West; OE: One Tree East; ON: One Tree North; IG: Inner Groove; OG: Outer Groove; RF: Reef Flat; IS:
 225 Inner Spur; OS: Outer Spur; SFR: Smooth fore reef; W: wide; N: narrow)

Location	Deployment	Site	Depth (m)	Approx. width (m)	Approx. spur wall height (m)	Dist. seaward of crest (m)	Dates	Site Descriptions/Comparisons
Moorea	Moorea North 1	MN1-IG	3.3	2	0.6	20	Aug to 9 Aug 2014	<ul style="list-style-type: none"> - Moderately exposed compared to other Moorea sites - SAG zone width ~100 m and gradient ~5° to a depth of ~12 m - Reef crest and flat submerged throughout the tidal cycle - Coral cover ~10-20% - Bottom of grooves are bare or have large, rounded rubble grading to patches of coarse sand with depth
		MN1-OG	9.1	5	4	90		
		MN1-RF	1.9	-	-	-		
	Moorea North 2	MN2-IG	3.3	2	0.6	20	11 Aug 2014	
		MN2-OG	8.9	5	4	90		
		MN2-OS	4.7	20	4	90		
		MN2-RF	1.9	-	-	-		
	Moorea East 1	ME1-IG	3.8	4	1.5	15	19 Aug to 20 Aug 2014	
		ME1-IS	2.7	6	1.5	18		
		ME1-OS	7.0	20	3	85		
	Moorea East 2	ME2-IG	3.8	4	1.5	15	21 Aug 2014	
		ME2-IS	2.7	6	1.5	18		
		ME2-OS	7.7	20	3	85		
Moorea North West	MNW-OG	5.8	1.5	2.5	54	15 Aug to 16 Aug 2014		
	MNW-RF _{SAG}	1.1	-	-	-			
	MNW-SFR	3.6	-	-	56			
	MNW-RF _{SFR}	1.4	-	-	-			

								rounded coral boulders - A 150 m long area of smooth fore reef (SFR) between SAGS
One Tree	One Tree East	OE-IG	2.8	1.5	1	28	11 Oct to 13 Oct 2013	<ul style="list-style-type: none"> - Most exposed of One Tree sites - SAG zone width ~120 m with gradient of ~2° to a depth of 6 m - classified as “exposed to wave energy” (EWE) by Duce et al. (2016) - Reef crest and flat exposed and therefore disconnected from SAGs over low tides - Coral cover ~75% - Bottom of grooves have large, smoothed rubble clasts transitioning to coarse rippled sand with depth
		OE-OG	5.4	2	2.5	88		
		OE-IS	1.9	7	1	28		
		OE-OS	2.5	10	2.5	88		
		OE-RF	0.6	-	-	-		
	One Tree North 1	ON1-IG _w	2.9	5.0	1.5	10	1 Dec 2014	<ul style="list-style-type: none"> - Least exposed of One Tree sites - SAG zone with ~200 m with gradient of ~4° to a depth of ~10 m
		ON1-OG _w	2.9	8.5	2.0	34		
		ON1-OG _N	2.1	1.5	1.0	29		
	One Tree North 2	ON2-IG _w	3.0	5.0	1.5	10	2 Dec to 3 Dec 2014	<ul style="list-style-type: none"> - Outer groove narrow (OGN) classified as “short and protected” (SaP); neighbouring wide groove (IGW and OGW) classified as “long and protected” (LaP) by Duce et al. (2016)
		ON2-OG _w	3.2	8.5	2.0	34		
		ON2-OG _N	2.4	1.5	1.0	29		
	One Tree North 3	ON3-IG _w	3.5	5.0	1.5	10	5 Jan 2015	<ul style="list-style-type: none"> - Reef crest and flat exposed and therefore disconnected from SAGs over low tides - Coral cover ~85%
		ON3-OG _w	3.6	8.5	2.0	34		
		ON3-OG _N	2.8	1.5	1.0	29		
	One Tree North 4	ON4-IG _w	3.5	5.0	1.5	10	7 Jan to 8 Jan 2015	<ul style="list-style-type: none"> - Bottom of the narrow groove and the outer end of the wider groove have poorly sorted, angular coral rubble and little sediment. Inner end of the wide groove has sand with some angular rubble and occasional live corals.
		ON4-OG _w				34		
				3.7	8.5	2.0		

226

227 3.3 Data Analysis

228 Spectral analysis of pressure sensor data was conducted using a Fourier transform
229 algorithm for 15-minute intervals with 50% overlap. A Hanning window was applied with
230 linear detrending. A dynamic pressure adjustment, based on Lee and Wang (1984), was
231 performed to account for pressure attenuation with depth and convert the subsurface pressure
232 record to surface waves. Linear wave theory has been shown to perform well in steep,
233 complex reef environments (Monismith et al., 2013). Thus, standard shallow water linear
234 wave theory was used to calculate the significant wave height (H_s) peak wave period (T_p)
235 and wave power (P).

236

$$P = 1/8\rho\rho gH_s^2Hs^2\sqrt{gh} \quad (1)$$

237

238

239 where, ρ is the density of sea water (1027 kg/m³), g is the gravitational acceleration
240 (9.81 m/s²) and h is water depth (m). Given the considerable number of deployments (10) and
241 instrument records (33) it is not practical to present the wave spectra or time series of wave
242 parameters for each instrument here. Instead, and to allow for comparison, we made box plots
243 in SPSS showing the median, first and third quartile of values recorded at each instrument
244 during each deployment.

245

246 We calculated energy dissipation rate per meter and percent of total energy dissipated
247 between outer and inner groove instruments and between inner groove and reef flat
248 instruments. Rates of wave energy dissipation (ϵ) in kilowatts per square meter (kW/m²)
249 were calculated using the following formula (based on Monismith et al. (2015)):

250

$$\epsilon = \frac{\Delta P}{\Delta x} \quad (2)$$

251

252 where, ΔP is the change in wave power (kW/m) between the outer and inner instruments and
253 Δx is the across reef distance in meters, between the two instruments. Following the findings
254 of Monismith et al. (2013), it was assumed that the direction of the incident wave field was
255 perpendicular to groove orientation. The effects of wave reflection were reported to be
256 minimal at a similar fore reef environment (Monismith et al., 2015) and therefore were not
257 considered. This method assumes wave energy is dissipated at a uniform rate between the
258 two instruments at which it is measured. While this is a reasonable assumption for unbroken

259 waves on the fore reef (OG-IG) when dissipation is due to bottom friction alone, it does not
260 hold when wave breaking occurs between two instruments. This is a limitation which must be
261 considered particularly when interpreting the dissipation rates calculated between the fore
262 reef and the reef flat (IG-RF).

263 To determine whether wave breaking would have been a factor in dissipating wave
264 energy we defined the wave breaking parameter such that:

265

$$\gamma = H_{max}/h \quad (3)$$

266

267 where, H_{max} is double H_s and h is water depth. Published wave breaking parameters
268 measured on coral fore reef environments vary from 0.83 (Rogers et al., 2016) to 0.98
269 (Monismith et al., 2013) up to 1.1 (Vetter et al., 2010). We chose a conservative estimation
270 (0.6) as we were interested in assessing the contribution of bottom friction to wave
271 dissipation in the absence of breaking, thus we needed to be sure that waves would not have
272 been breaking at our fore reef instruments.

273

274 **4. Results**

275 **4.1 Offshore wave and wind conditions**

276 4.1.1 Moorea

277 During the study period in August 2014 the offshore wave climate at Moorea, obtained from
278 WW3, was dominated by south, southwesterly swell with mean significant wave height of 2.0
279 m (Supp. Figure 1). The waves recorded at FOR01 on the northern reef had a mean H_s of
280 0.6 m, a maximum H_s of 1.2 m and a T_p of 8 seconds. Waves approached from a northerly
281 direction (Supp. Figure 1 c) suggesting that the offshore waves obtained from the WW3
282 model had refracted around the northern side of the island. Local winds at Moorea have
283 previously been reported to have minimal effects on hydrodynamic circulation and thus were
284 not examined in this study (Hench et al., 2008).

285 4.1.2 One Tree

286 The mean offshore significant wave height during the One Tree East deployment (11-13 Oct
287 2013) was 0.78 m with a maximum H_s of 1.1 m and T_p of 5 s (Supp. Figure 2). During this
288 deployment the offshore wave direction was north-northeasterly, and winds were northerly.
289 During the One Tree North deployments (Nov 2014 to Jan 2015) the mean offshore H_s was

290 1.5 m with a maximum H_s of 3.4 m and a T_p of 7 seconds. Waves were predominately from
291 the east (Figure 4c). The average maximum wind speed during One Tree North deployments
292 was 29 km/h from an easterly direction (Supp. Figure 3d). During One Tree North
293 deployment 4 (7-8 Jan 2015) there was a relatively high energy event with maximum
294 offshore H_s reaching 3 m and a maximum wind speed (i.e., the highest speed recorded each
295 30 min period) of 54 km/h from the east (Supp. Figure 3e).

296

297 **4.2 Wave conditions in the SAG zone**

298 Measured mean H_s were relatively small (<1 m) during all deployments with wave conditions
299 during each deployment varying across the SAG zone (Figure 3). Spectral analysis revealed
300 the dominant energy component to be the incident frequency band (3-25 s) for all
301 deployments. Time series of wave conditions for all deployments are provided in the
302 Supplementary material (Supp. Figures 4-13). The conservative wave breaking parameter
303 was exceeded only at the outer and inner spurs, and the inner groove at One Tree East during
304 part of the first low tide. No other instruments showed wave breaking though it is assumed
305 that breaking would have occurred at the reef crest between the inner SAG instruments and
306 the reef flat instruments.

307 P was greatest at the deepest and furthest seaward instruments (usually outer groove
308 instruments) for all deployments (Figure 3). The largest waves (mean $H_s = 0.86$ m, $P =$
309 7kW/m) were recorded at the outer groove at Moorea North West (Figure 3 e, o), followed by
310 both spurs and grooves at One Tree East (Figure 3f, p) and Moorea East 2 (Figure 3d, n). The
311 smallest and least powerful waves for all deployments were recorded at the reef flat
312 instruments. Regardless of wave height offshore, under modal conditions such as those
313 recorded, virtually all power and height was dissipated by the time the waves reached the reef
314 flat.

315 When comparing data from adjacent inner spur and inner groove we found that at Moorea
316 East mean H_s and P for both deployments were higher at the spur (up to 2.61 kW/m) than the
317 groove (up to 2.15 kW/m, Figure 3m, n), which could be related to increased shoaling over
318 the spurs. Conversely, at One Tree East the inner groove had slightly higher H_s and P (2
319 kW/m) than the adjacent inner spur (1.6 kW/m) (Figure 3p). The instruments were
320 approximately one meter shallower than at Moorea East (OE inner spur depth 1.9 m and
321 groove 2.9 m vs 2.7 m and 3.8 m at ME) (Table 1), suggesting that as waves propagate

322 further across the SAG zone, bottom friction influences waves at the spur more than the
 323 groove. At sites where we conducted more than one deployment (i.e., MN, ME and ON)
 324 despite changes in the magnitude of H_s and P the pattern of wave characteristics within the
 325 zone was consistent between deployments (e.g., at ME power was highest at the outer spur,
 326 followed by the inner spur then the inner groove).

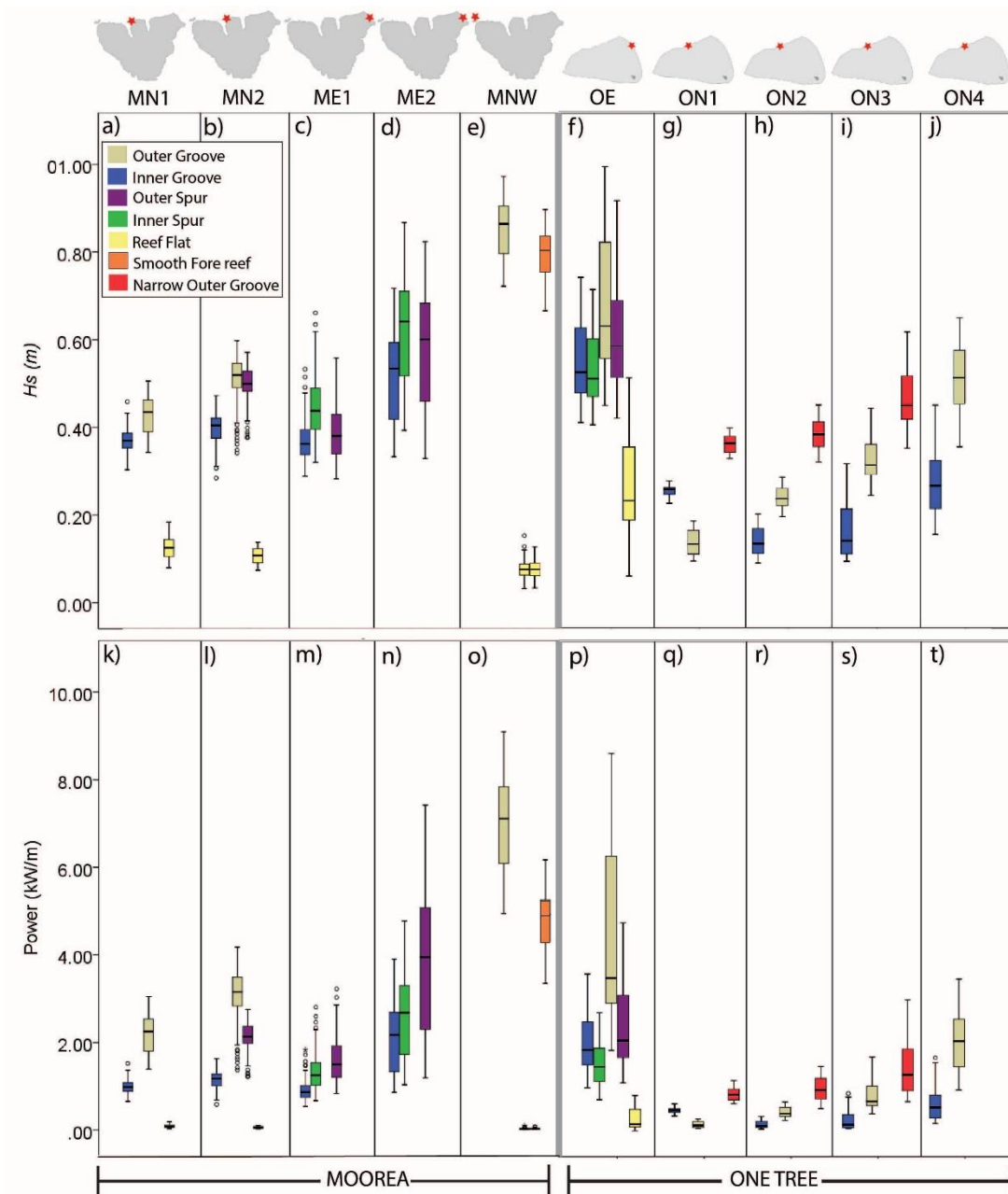


Figure 3 Comparison of box plots showing H_s (a-j) and P (k-t) throughout all deployments. The colour of each box plot denotes the location of the instrument at the inner or outer groove, inner or outer spur, narrow outer groove, smooth fore reef or reef flat. Each panel is one deployment as labeled at the top. Panels a) to e) and k) to o) are Moorea deployments while f) to j) and p) to t) are One Tree deployments. Box plots show the median, first and third quartile of values recorded at each instrument during each deployment.

327 4.3 Wave energy dissipation

328 We found considerable variation in dissipation rates both between and within deployments.
329 For example, the highest dissipation rate measured at One Tree East (0.1 kW/m^2 between the
330 outer and inner groove) was ten times higher than the lowest dissipation rate (0.01 kW/m^2)
331 between the same instruments during the same deployment (Figure 4g). The dissipation rates
332 between the outer and inner groove were higher at the One Tree sites (OE mean $\epsilon = 0.04$
333 kW/m^2 ; ON = 0.06 kW/m^2) than the Moorea sites (MN1 mean $\epsilon = 0.02 \text{ kW/m}^2$; MN2 = 0.03
334 kW/m^2) (Figure 4e-h). Interestingly, at both Moorea and One Tree, the rate of energy
335 dissipation on the fore reef between the outer and inner groove was always higher than
336 between the inner groove and the reef flat (Figure 4e-g). The greatest difference was at
337 Moorea North during deployment 2 where the mean dissipation rate across the groove (mean
338 $\epsilon = 0.03 \text{ kW/m}^2$) was six times higher than across the reef crest (mean $\epsilon = 0.005 \text{ kW/m}^2$). One
339 Tree East was the only site where direct comparison of dissipation of across an adjacent spur
340 and groove was possible. Somewhat surprisingly the measured dissipation rate across a
341 groove (max = 0.1 kW/m^2 ; mean = 0.04 kW/m^2) was almost three times that across the
342 adjacent spur (max = 0.048 kW/m^2 ; mean = 0.014 kW/m^2) (Figure 4g). This difference was
343 most pronounced at high tide.

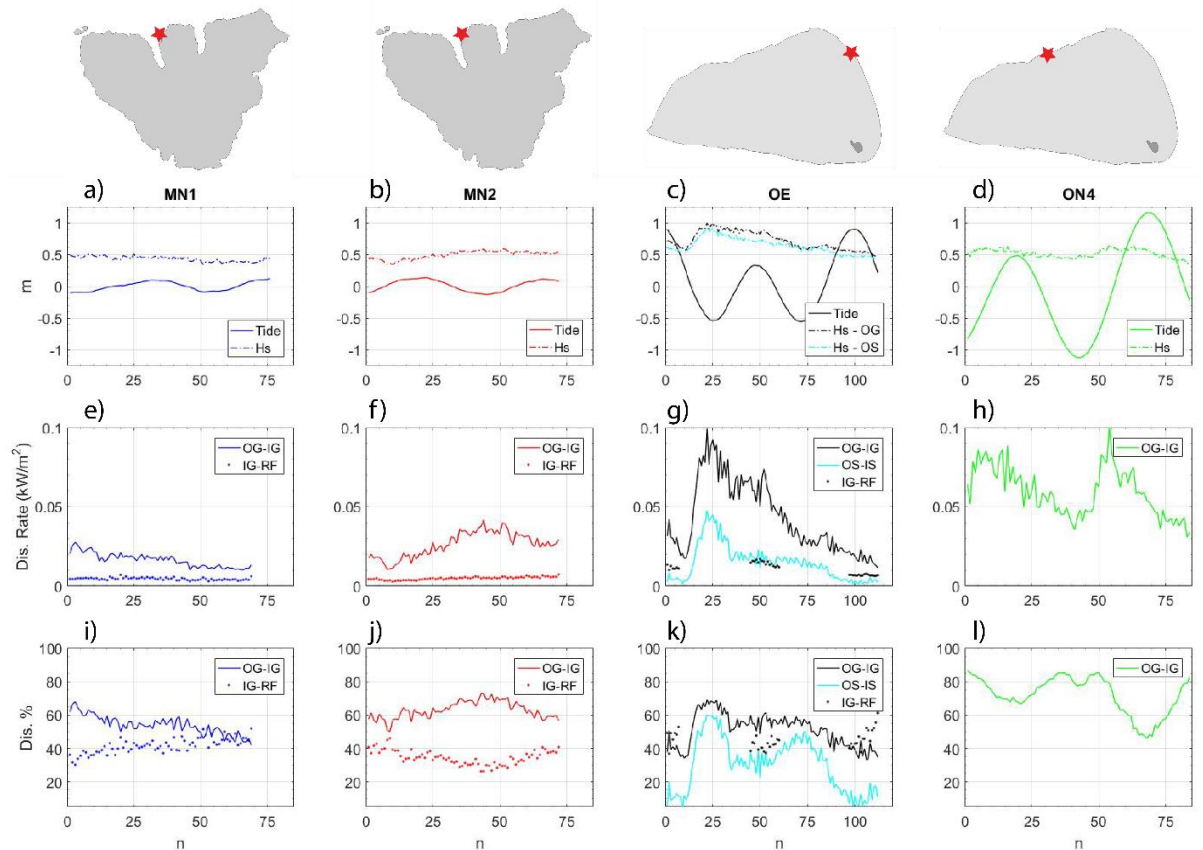
344

345 Most of the time the percentage of energy dissipated across the SAG zone was greater
346 than that dissipated across the reef crest (Figure 4i-k). The maximum percentage of wave
347 energy dissipated between the outer and inner groove was 86% at One Tree North
348 Deployment 4 (Figure 4l) while the maximum dissipation across the reef crest was 62% at
349 One Tree East (Figure 4k). During high tides and low wave energy conditions at Moorea
350 North Deployment 1 and One Tree East (Figure 4i and k) the percentage dissipated across the
351 reef crest equaled or briefly exceeded the percent dissipated across the SAG zone. During all
352 deployments, the greatest percentage of energy dissipated by the SAG zone was during low
353 tides with relatively high wave conditions.

354 The wave energy dissipation increased more sharply with H_s across the SAG zone than
355 across the reef crest (Figure 5a-c). At Moorea North Deployments 1 and 2 and One Tree East
356 percent dissipation across the SAG zone was also significantly positively correlated with H_s
357 (Figure 5e-g). In contrast, percent dissipation was significantly negatively correlated with H_s
358 across the reef crest. Percent dissipation and H_s were also negatively correlated between the
359 wide outer and inner groove at One Tree North (Figure 5h). Across the SAG zone there is a
360 significant negative correlation between percent dissipation and depth at all sites while across

361 the reef crest it is positively correlated at Moorea North but there is no relationship at One
 362 Tree East (Figure 5i-k). The positive correlation between dissipation percent and H_s across the
 363 fore reef and negative correlation across the reef crest suggest bottom friction at the fore reef
 364 becomes more important for energy dissipation as wave height increases.

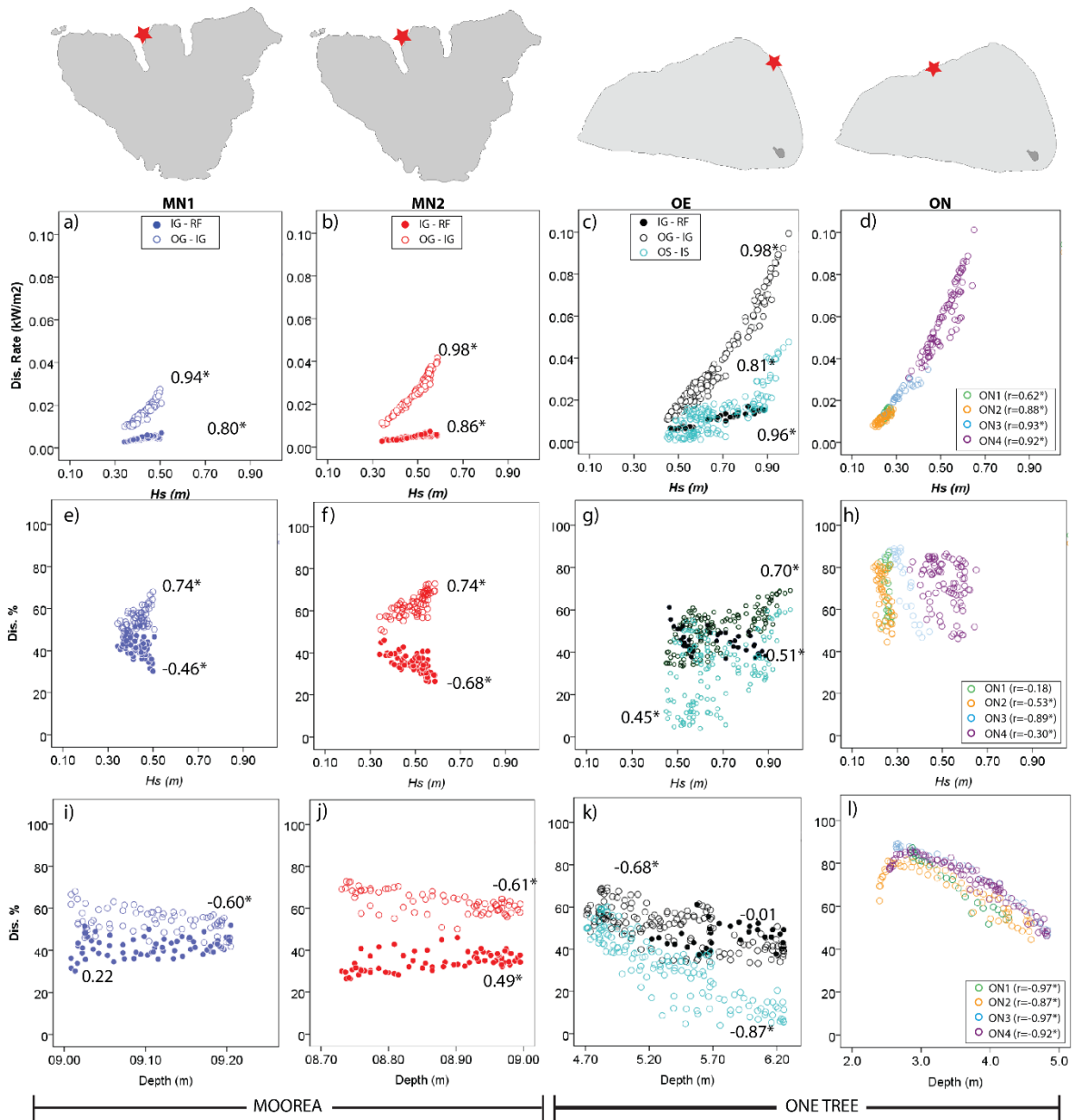
365
 366



367

Figure 4 Wave dissipation characteristics at Moorea North deployments 1 and 2 (MN1, MN2), One Tree East (OE) and One Tree North deployment 4 (ON4). Panels a) to d) show tidal stage and H_s . The rates of wave power dissipation per meter from the outer groove to the inner groove (OG – IG unbroken line) and the inner groove to the reef flat (IG – RF dotted line) are shown in panels e) to h). Note that ON4 (h) does not have IG-RF as no instrument was deployed on the reef flat. Panels i) to l) show the percentage of wave power dissipated from OG-IG (unbroken line) and IG-RF (dotted line). The x-axis is number of records, where each record accounts for 15 minutes. The reef flat at OE is sub-aerially exposed over low tidal phases therefore IG-RF calculations could only be made over high tides when waves could propagate across the reef crest. Note that deployments were not concurrent.

368



369
 370 **Figure 5** Relationships between dissipation rate and H_s (a-d); percent of energy dissipated
 371 and H_s (e-h) and; percent of energy dissipated and depth (i-l) across the SAG zone from outer
 372 to inner groove (open symbols) and from inner groove to reef flat (filled symbols) at MN1,
 373 MN2, OE and ON4. Pearson's correlation r values are given with an asterisk denoting
 374 significance at the 95% level and minus signs denoting a negative correlation. Note that the
 375 x-axes of plots i-l do not have the same scale.
 376

377 5 Discussion

378 5.1 Wave energy dissipation across the SAG zone vs the reef crest

379 Our study is one of the first to measure dissipation across the fore reef SAG zone and the reef
 380 crest and compare the relative importance of bottom friction and wave breaking. We found
 381 that SAG zones at Moorea and One Tree Reef dissipated between 33 to 86% of wave energy
 382 at extremely high rates (up to 0.01 - 0.1 kW/m²) through bottom friction alone (Figure 4e-g).

383 We found rates of wave energy dissipation across the SAG zone between the outer and inner
384 groove, due to bottom friction, were between four and six times higher than across the reef
385 crest where breaking likely contributed to energy dissipation (Figure 4e-h). The percentage of
386 energy dissipated across the SAG zone was also higher than across the reef crest most of the
387 time (Figure 4i-l). These findings call into question the long-held assumption that the vast
388 majority of wave energy dissipation occurs at the reef crest (Ferrario et al., 2014). The
389 importance of dissipation at the fore reef was also reported by Monismith et al. (2015) who
390 measured rates of wave energy dissipation up to 0.03 kW/m^2 on the fore reef between 11.2
391 and 6.2 m depth at Palmyra Atoll and calculated an extremely high wave friction factor
392 (1.80). A calibrated SWAN model for the same reef also found that the average wave
393 dissipation rates at the fore reef due to bottom friction were larger than those due to wave
394 breaking (Rogers et al., 2016).

395

396 We found significant positive correlations between percentage of energy dissipation and H_s
397 across the fore reef (Figure 5e-g) and negative correlations across the reef crest. This suggests
398 that, under the modal wave conditions measured, bottom friction at the fore reef is
399 increasingly important for energy dissipation as wave height increases. This is somewhat
400 consistent with modelling by Lowe et al. (2005) at Kaneohe Bay, Hawaii predicting that fore
401 reef dissipation due to bottom friction would be greater than dissipation due to wave breaking
402 under lower-than-average wave heights and approximately equal for average incident wave
403 heights. For larger than average waves, their model predicted that wave breaking would
404 become more important and dissipate energy at approximately double the rate of bottom
405 friction. The wave heights during all our deployments were average or below average and we
406 found rates of dissipation at the fore reef to be between 4 and 6 times the rates of dissipation
407 across the reef crest (Figure 4e-h).

408

409 In addition to wave height, we found water depth (i.e., tidal stage) to be important in
410 determining wave energy dissipation across the fore reef compared to the reef crest. We
411 found that as water depth increased, the percentage of energy dissipated across the SAG zone
412 decreased, while the percentage dissipated across the reef crest increased (Figure 5i-l). Thus,
413 even in micro-tidal Moorea (MN1 and MN2), tidal stage played a role in the relative
414 percentage of energy dissipated across the SAG zone as compared to the reef crest. Tidal
415 modulation of the wave field at Moorea was also noted by Monismith et al. (2013). The
416 decline in percent of energy dissipation with increasing water depth was particularly

417 pronounced at One Tree North where half as much wave energy was dissipated at high tides
418 compared to low tides (Figure 51). This agrees with previous findings on how propagation is
419 controlled by tidal stage at One Tree Reef (Harris et al., 2015; Vila-Concejo et al., 2014).

420

421 The correlations we measured between percentage dissipation, H_s and water depth provide
422 general insights into the functioning of the fore reef and reef crest and allow us to draft a
423 conceptual model (Figure 6). Under high wave conditions and low tides the proportion of
424 dissipation is greater at the fore reef than the reef crest because the wave base interacts with
425 the rough and topographically complex fore reef SAGs and dissipates the majority of its
426 energy as bottom friction before it reaches the crest. Conversely, under low wave conditions
427 and deep water (high tides) the wave base does not reach the bed at the fore reef and more
428 energy is dissipated at the crest. Under high wave conditions and deep water, the reef crest
429 becomes more important, with waves breaking across the SAG as suggested by Lowe et al.
430 (2005) and da Silva et al. (2020). At Moorea North our data showed that when H_s was less
431 than 0.5 m and water depth was approximately 0.1 m above MSL the proportions of wave
432 energy dissipated at the fore reef and reef crest were approximately equal. While at One Tree
433 East this occurred when water depths were ~1 m above MSL and H_s was <0.75 m. Our
434 findings that the percentage of energy dissipation at the fore reef declines with increasing
435 depth agree with studies linking sea level rise to an increased risk of wave attack and erosion
436 for islands and coasts currently protected by coral reefs (e.g., Albert et al. (2016), Quataert et
437 al. (2015), Storlazzi et al. (2015) and Storlazzi et al. (2011)).

438

439

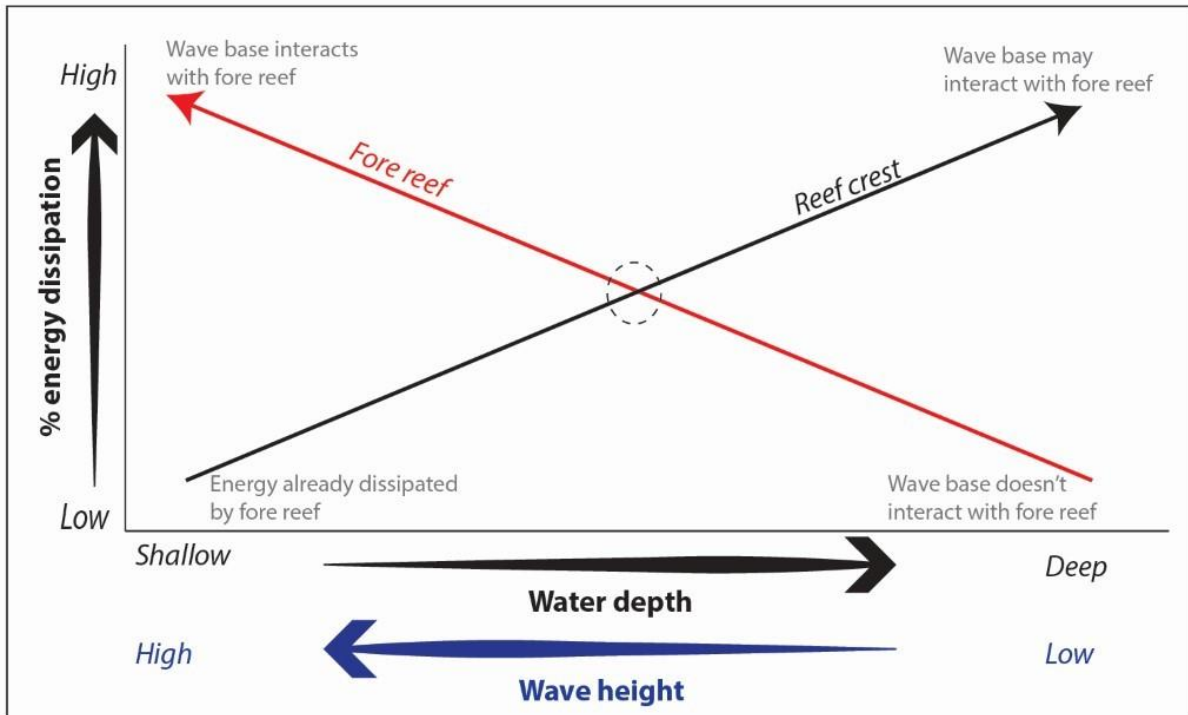


Figure 6 Conceptual model depicting the relative percentage of wave energy dissipated at the fore reef (red line) and reef crest (black line) under different wave height and water depth conditions. Our measurements at Moorea North and One Tree East allowed us to define the water depths and wave heights at which the fore reef and reef crest will dissipate approximately equal percentages of incoming wave energy (dashed circle).

440

441 **5.2 Global comparison of fore reef dissipation rates**

442 An extensive literature review only found four other studies measuring wave conditions at
 443 more than one station on the fore reef allowing for calculation of fore reef wave dissipation
 444 rates (Monismith et al., 2013; Monismith et al., 2015; Pequignet et al., 2011; Storlazzi et al.,
 445 2004). The dissipation rates presented in our study are comparable to other reefs globally
 446 (Figure 7). However, one should consider that mean dissipation rate is an imperfect metric as
 447 our results demonstrate that dissipation rates are highly spatially and temporally variable and
 448 dependent on offshore wave conditions during the deployment. The highest mean dissipation
 449 rate measured across the SAG zone in this study was at One Tree North Deployment 4, on the
 450 relatively shallow, leeward side (mean $\epsilon = 0.056 \text{ kW/m}^2$). Monismith et al. (2015) suggested
 451 that the relatively high dissipation rate ($\sim 0.02 \text{ kW/m}^2$) and wave friction factor (1.8)
 452 measured at the relatively deep (11- 6 m) fore reef in Palmyra Atoll were due to high levels
 453 of live, healthy coral cover. Our study provides initial evidence to support this. Generally, we
 454 measured higher rates of dissipation across the fore reef SAG zone at One Tree (ON and OE)
 455 than at Moorea (MN1 and MN2) and the levels of live coral cover between the sites differed
 456 considerably (ON= $\sim 85\%$, OE= $\sim 70\%$, MN=10-20%). The spurs were higher at Moorea North

457 than either of the One Tree sites (refer to Table 1) and the fore reef gradients at these sites
 458 were similar (ON=4°, OE=2° and MN=5°) thus it is unlikely that slope drove the difference
 459 in dissipation rates. The larger tidal range at One Tree and the associated tidal currents are
 460 also likely to play a role in wave dissipation and implies that tidal currents are likely to be an
 461 important factor modulating wave energy dissipation in meso and particularly macro tidal
 462 environments.
 463 One Tree North may also experience offshore currents driven by wave pumping of the type
 464 reported by Callaghan et al. (2006); and Nielsen et al. (2008) whereby waves on the exposed
 465 side of the reef push water into and across the lagoon and it drains out on the leeward side.
 466 Indeed, there was greater variability in the instantaneous velocity of currents at One Tree
 467 North than at Moorea North (Duce, 2017). Further research is warranted to assess the
 468 influence of tidal currents, wave pumping, and live coral cover at the fore reef on wave
 469 energy dissipation. More data is required from multiple fore reef instrument arrays to better
 470 understand the important role of this understudied geomorphic zone in dissipating wave
 471 energy.
 472

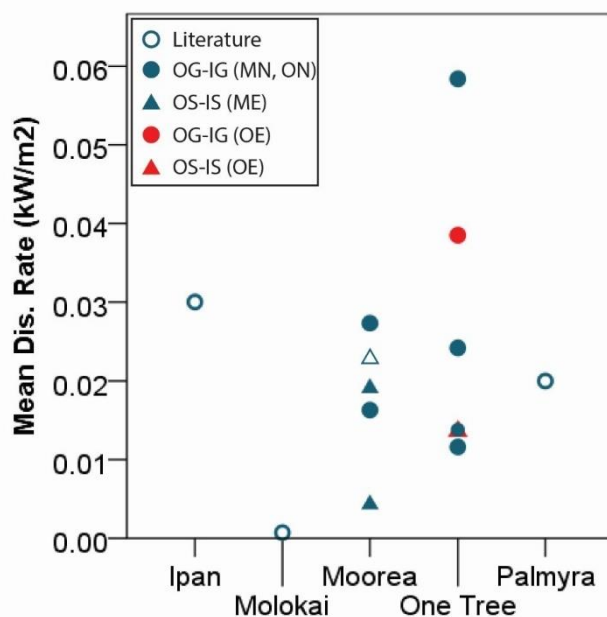


Figure 7 Mean dissipation rates (kW/m²) of wave energy across the fore reef at different sites globally. Filled symbols are deployments Moorea north (MN), One Tree north (ON), Moorea east (ME) and One Tree east (OE) with circles representing measurements between the outer and inner groove and triangles representing measurements between the outer and inner spur. Filled symbols represent measurements obtained in this study while open symbols represent values obtained from the literature. The reefs at which these rates were measured are shown on the x-axis with data derived from the following sources: Ipan, Guam (Pequignet et al., 2011); Molokai (Storlazzi et al., 2004); Moorea (this study and (Monismith et al., 2013); One Tree (this study); Palmyra Atoll (Monismith et al., 2015).

474 **5.3 Comparison of wave dissipation with other ecosystems**

475 Coral reefs provide important ecosystem services in protecting the coasts from incoming
476 wave energy (Ferrario et al., 2014). While direct comparison is not always possible due to
477 different methods of calculating wave dissipation, authors have shown that mangroves in
478 Vietnam could reduce wave energy between 1.7 to 6% for every 10 m (Barbier et al., 2008).
479 More recently, Gon et al. (2020) showed that a rock platform off Monterey Bay in California
480 (USA) dissipated 32% over 132 m (i.e., 2.4% of the energy over 10 m). While most previous
481 studies in reef environments presented wave dissipation over reef flats, this paper highlights
482 the high amount of wave dissipation that occurs over the SAG on the fore reef and underlines
483 the importance of accounting for this in future numerical modelling studies. Our results show
484 SAG maximum (minimum) dissipation percentages over 10 m of 10.4% (6%) in Moorea and
485 35.9% (20.2%) at One Tree Reef. While we did not obtain detailed bathymetric data to obtain
486 roughness or friction factors, our results demonstrate that coral reefs, and in particular SAGs,
487 are amongst the most effective natural wave dissipaters on Earth. Temmerman et al. (2013)
488 claimed that flood protection by ecosystem creation and restoration could provide a
489 sustainable and cost-effective coastal engineering solution and called for implementation
490 when possible. The coastal protection services provided by coral reefs demand global
491 attention and conservation in light of ongoing climate change.

492

493 Numerical modelling has suggested that the structural complexity of coral reefs is more
494 important than sea-level rise in determining the level of coastal protection provided by reefs
495 under average wave conditions (Harris et al., 2018). An important future avenue for research
496 includes coupling high spatial resolution (centimeter to meter scales) mapping of the 3D
497 structure (rugosity) of reef environments (particularly the difficult to reach fore reef zone)
498 with closely spaced instrument transects to gain an in-depth understanding of local scale
499 turbulence and friction induced by the interaction between coral reefs with differing benthic
500 cover and hydrodynamic forces (waves and currents).

501 **6. Conclusions**

502 We measured waves and currents in the fore reef spur and groove zone during a range of
503 modal conditions at Moorea, French Polynesia and One Tree Reef, southern GBR, Australia.
504 The study sites chosen had contrasting tides (micro and meso), wave regimes (exposed and
505 sheltered), broad scale reef type (barrier reef and lagoonal platform reef), local fore reef SAG

506 morphology and levels of live coral cover. We found extremely high rates of wave energy
507 dissipation (up to 0.1 kW/m²) across the fore reef SAG zone due to bottom friction alone (i.e.,
508 no component of wave breaking). Under the modal conditions measured, the percent of
509 energy dissipated at the fore reef was almost always higher than the percent dissipated across
510 the reef crest, calling into question the dominant assumption that the reef crest is the most
511 important geomorphic zone for energy dissipation. A conceptual model was developed
512 showing that fore reef dissipation is more important than reef crest dissipation under high
513 wave conditions at low tides, while reef crest dissipation is more important at high tides and
514 small waves. In general, higher rates of dissipation were measured across SAG zones at One
515 Tree Reef than Moorea. This may support claims that higher live coral cover produces greater
516 bottom friction and wave dissipation though more research is required. It also suggests the
517 importance of tidal currents in influencing wave energy dissipation. Longer deployments,
518 capturing a range of hydrodynamic driving conditions, with instruments at inner and outer
519 ends of both spurs and grooves are required to better understand the complex nature of
520 morphodynamic feedbacks in this important zone.

521

522 **Acknowledgements**

523 We gratefully acknowledge funding from a Tempe Mann Travelling Scholarship from the
524 Australian Federation of Graduate Women (S.D.), an Australian Postgraduate Award (S.D.),
525 a University of Sydney Merit Award (S.D), a Great Barrier Reef Marine Park Authority
526 Science for Management Award (S.D. 9/1667(2)) an ARC Future Fellowship (A.V.C.,
527 FT100100215) and return to work grant for Women in Science at the University of Sydney
528 (AVC). We also thank staff at CRIOBE research station and One Tree Island Research
529 Station. The help of field volunteers Russell Graham, Glen Shaw, Matt Kosnik, Andrew
530 Irving, Pepe Brennen, Vetea Liao, Andrew Durrant, Selma Klanten, Jonathan Walsh and
531 Aero Leplastrier is greatly appreciated. Offshore wave data sets were provided by the Moorea
532 Coral Reef Ecosystem Long-Term Ecological Research (LTER) program, funded by the US
533 National Science Foundation (OCE-0417412) and the Queensland Integrated Marine
534 Observing System (Q-IMOS) operated by the Australian Institute of Marine Science with the
535 assistance of Craig Steinberg. Datasets for this research are available from Figshare:
536 [https://figshare.com/articles/dataset/SAG_Hydrodynamics_Datasets_Moorea_and_One_Tree/
537 14036747](https://figshare.com/articles/dataset/SAG_Hydrodynamics_Datasets_Moorea_and_One_Tree/14036747).

538

539 **References**

540 Adjeroud, M., Michonneau, F., Edmunds, P. J., Chancerelle, Y., de Loma, T. L., Penin, L., . . . Galzin, R.
541 (2009). Recurrent disturbances, recovery trajectories, and resilience of coral assemblages on
542 a South Central Pacific reef. *Coral Reefs*, 28(3), 775-780. doi:10.1007/s00338-009-0515-7

543 Albert, S., Leon, J. X., Grinham, A. R., Church, J. A., Gibbes, B. R., & Woodroffe, C. D. (2016).
544 Interactions between sea-level rise and wave exposure on reef island dynamics in the
545 Solomon Islands. *Environmental Research Letters*, 11(5), 1-9.

546 Baldock, T. E., Shabani, B., & Callaghan, D. P. (2019). Open access Bayesian Belief Networks for
547 estimating the hydrodynamics and shoreline response behind fringing reefs subject to
548 climate changes and reef degradation. *Environmental Modelling and Software*, 119(June),
549 327-340. doi:10.1016/j.envsoft.2019.07.001

550 Baldock, T. E., Shabani, B., Callaghan, D. P., Hu, Z., & Mumby, P. J. (2020). Two-dimensional
551 modelling of wave dynamics and wave forces on fringing coral reefs. *Coastal Engineering*,
552 155. doi:10.1016/j.coastaleng.2019.103594

553 Barbier, E. B., Koch, E. W., Silliman, B. R., Hacker, S. D., Wolanski, E., Primavera, J., . . . Reed, D. J.
554 (2008). Coastal ecosystem-based management with nonlinear ecological functions and
555 values. *Science*, 319(5861), 321-323. doi:10.1126/science.1150349

556 Beck, M. W., Losada, I. J., Menéndez, P., Reguero, B. G., Díaz-Simal, P., & Fernández, F. (2018). The
557 global flood protection savings provided by coral reefs. *Nature Communications*, 9(1).
558 doi:10.1038/s41467-018-04568-z

559 Beetham, E. P., & Kench, P. S. (2014). Wave energy gradients and shoreline change on Vabbinfaru
560 platform, Maldives. *Geomorphology*, 209, 98-110. doi:10.1016/j.geomorph.2013.11.029

561 Bramante, J. F., Ashton, A. D., Storlazzi, C. D., Cheriton, O. M., & Donnelly, J. P. (2020). Sea-level rise
562 will drive divergent sediment transport patterns on fore reefs and reef flats, potentially
563 causing erosion on atoll islands. *Journal of Geophysical Research: Earth Surface*.
564 doi:10.1029/2019jf005446

565 Brander, R. W., Kench, P. S., & Hart, D. (2004). Spatial and temporal variations in wave characteristics
566 across a reef platform, Warraber Island, Torres Strait, Australia. *Marine Geology*, 207(1-4),
567 169-184. doi:10.1016/j.margeo.2004.03.014

568 Bryson, M., Duce, S., Harris, D., Webster, J. M., Thompson, A., Vila-Concejo, A., & Williams, S. B.
569 (2016). Geomorphic changes of a coral shingle cay measured using Kite Aerial Photography.
570 *Geomorphology*, 270, 1-8. doi:10.1016/j.geomorph.2016.06.018

571 Callaghan, D. P., Nielsen, P., Cartwright, N., Gourlay, M. R., & Baldock, T. E. (2006). Atoll lagoon
572 flushing forced by waves. *Coastal Engineering*, 53(8), 691-704.
573 doi:<http://dx.doi.org/10.1016/j.coastaleng.2006.02.006>

574 Cheriton, O. M., C. D. Storlazzi and K. J. Rosenberger (2016). "Observations of wave transformation
575 over a fringing coral reef and the importance of low-frequency waves and offshore water
576 levels to runup, overwash and coastal flooding." *Journal of Geophysical Research: Oceans*
577 121.

578 da Silva, R. F., Storlazzi, C. D., Rogers, J. S., Reynolds, J., & McCall, R. (2020). Modelling three-
579 dimensional flow over spur-and-groove morphology. *Coral Reefs*. doi:10.1007/s00338-020-
580 02011-8

581 Duce, S. (2017). *The Form, Function and Evolution of Coral Reef Spur and Grooves*. (Unpublished PhD
582 Thesis). University of Sydney, Sydney, Australia.

583 Duce, S., Dechnik, B., Webster, J. M., Hua, Q., Sadler, J., Webb, G. E., . . . Vila-Concejo, A. (2020).
584 Mechanisms of spur and groove development and implications for reef platform evolution.
585 *Quaternary Science Reviews*, 231, 106155.
586 doi:<https://doi.org/10.1016/j.quascirev.2019.106155>

587 Duce, S., Vila-Concejo, A., Hamylton, S. M., Webster, J. M., Bruce, E., & Beaman, R. J. (2016). A
588 morphometric assessment and classification of coral reef spur and groove morphology.
589 *Geomorphology*, 265, 68-83.

590 Edmunds, P. J., & Leichter, J. J. (2016). Spatial scale-dependent vertical zonation of coral reef
591 community structure in French Polynesia. *Ecosphere*, 7(5), 1-14. doi:10.1002/ecs2.1342

592 Etienne, S. (2012). Marine inundation hazards in French Polynesia: Geomorphic impacts of tropical
593 cyclone oli in February 2010. *Geological Society Special Publication*, 361(1), 21-39.
594 doi:10.1144/SP361.4

595 Ferrario, F., Beck, M. W., Storlazzi, C. D., Micheli, F., Shepard, C. C., & Airoidi, L. (2014). The
596 effectiveness of coral reefs for coastal hazard risk reduction and adaptation. *Nature*
597 *Communications*, 5, 3794. doi:10.1038/ncomms4794

598 Foley, M., Stender, Y., Singh, A., Jokiel, P., & Rodgers, K. u. (2014). Ecological Engineering
599 Considerations for Coral Reefs in the Design of Multifunctional Coastal Structures. *Coastal*
600 *Engineering Proceedings*, 1(34), 30-30. doi:10.9753/icce.v34.management.30

601 Frith, C. A., & Mason, L. B. (1986). Modelling wind driven circulation One Tree Reef, Southern Great
602 Barrier Reef. *Coral Reefs*, 4(4), 201-211. doi:10.1007/BF00298078

603 Gallop, S. L., Young, I. R., Ranasinghe, R., Durrant, T. H., & Haigh, I. D. (2014). The large-scale
604 influence of the Great Barrier Reef matrix on wave attenuation. *Coral Reefs*, 33(4), 1167-
605 1178. doi:10.1007/s00338-014-1205-7

606 Gischler, E. (2010). Indo-Pacific and Atlantic spurs and grooves revisited: The possible effects of
607 different Holocene sea-level history, exposure, and reef accretion rate in the shallow fore
608 reef. *Facies*, 56(2), 173-177. doi:10.1007/s10347-010-0218-0

609 Gon, C. J., MacMahan, J. H., Thornton, E. B., & Denny, M. (2020). Wave Dissipation by Bottom
610 Friction on the Inner Shelf of a Rocky Shore. *Journal of Geophysical Research: Oceans*,
611 125(10). doi:10.1029/2019jc015963

612 Hamylton, S., Silverman, J., & Shaw, E. (2013). The use of remote sensing to scale up measures of
613 carbonate production on reef systems: a comparison of hydrochemical and census-based
614 estimation methods. *International Journal of Remote Sensing*, 34(18), 6451-6465.
615 doi:10.1080/01431161.2013.800654

616 Hardy, T. A., & Young, I. R. (1996). Field study of wave attenuation on an offshore coral reef. *Journal*
617 *of Geophysical Research: Oceans*, 101(C6), 14311-14326. doi:10.1029/96JC00202

618 Harris, D. L., Rovere, A., Casella, E., Power, H. E., Canavesio, R., Collin, A., . . . Parravicini, V. (2018).
619 Coral reef structural complexity provides important coastal protection from waves under
620 rising sea levels. *Science Advances*, 4(2), 1-7. doi:10.1126/sciadv.aao4350

621 Harris, D. L., & Vila-Concejo, A. (2013). Wave transformation on a coral reef rubble platform. *Journal*
622 *of Coastal Research*, 65, 506-510. doi:10.2112/si65-086.1

623 Harris, D. L., Vila-Concejo, A., Webster, J. M., & Power, H. E. (2015). Spatial variations in wave
624 transformation and sediment entrainment on a coral reef sand apron. *Marine Geology*, 363,
625 220-229. doi:10.1016/j.margeo.2015.02.010

626 Hench, J. L., Leichter, J. J., & Monismith, S. G. (2008). Episodic circulation and exchange in a wave-
627 driven coral reef and lagoon system. *Limnology and Oceanography*, 53(6), 2681-2694.
628 doi:10.4319/lo.2008.53.6.2681

629 Hopley, D., Smithers, S. G., & Parnell, K. E. (2007). *The Geomorphology of the Great Barrier Reef :*
630 *development, diversity, and change*. Cambridge: Cambridge University Press.

631 Horstman, E. M., Dohmen-Janssen, C. M., Narra, P. M. F., van den Berg, N. J. F., Siemerink, M., &
632 Hulscher, S. J. M. H. (2014). Wave attenuation in mangroves: A quantitative approach to
633 field observations. *Coastal Engineering*, 94, 47-62. doi:10.1016/j.coastaleng.2014.08.005

634 Huang, Z. C., Lenain, L., Melville, W. K., Middleton, J. H., Reineman, B., Statom, N., & McCabe, R. M.
635 (2012). Dissipation of wave energy and turbulence in a shallow coral reef lagoon. *Journal of*
636 *Geophysical Research: Oceans*, 117(3), 1-18. doi:10.1029/2011JC007202

637 Kayal, M., Vercelloni, J., Lison de Loma, T., Bosserelle, P., Chancerelle, Y., Geoffroy, S., . . . Adjeroud,
638 M. (2012). Predator Crown-of-Thorns Starfish (*Acanthaster planci*) Outbreak, Mass Mortality
639 of Corals, and Cascading Effects on Reef Fish and Benthic Communities. *PLoS ONE*, 7(10).
640 doi:10.1371/journal.pone.0047363

641 Kench, P. S., & Brander, R. W. (2006). Wave Processes on Coral Reef Flats: Implications for Reef
642 Geomorphology Using Australian Case Studies. *Journal of Coastal Research*, 221, 209-223.
643 doi:10.2112/05a-0016.1

644 Kench, P. S., Brander, R. W., Parnell, K. E., & O'Callaghan, J. M. (2009). Seasonal variations in wave
645 characteristics around a coral reef island, South Maalhosmadulu atoll, Maldives. *Marine*
646 *Geology*, 262(1-4), 116-129. doi:10.1016/j.margeo.2009.03.018

647 Lee, D.-Y., & Wang, H. (1984). Measurement of surface waves from subsurface gage. *Coastal*
648 *Engineering Proceedings*, 1(19), 271-286.

649 Leichter, J. J., Alldredge, A. L., Bernardi, G., Brooks, A. J., Carlson, C. A., Carpenter, R. C., . . . Wyatt, A.
650 S. J. (2013). Biological and Physical Interactions on a Tropical Island Coral Reef: Transport
651 and Retention Processes on Morea, French Polynesia. *Oceanographic Society*, 26(3), 52-63.

652 Leichter, J. J., Stokes, M. D., Hench, J. L., Witting, J., & Washburn, L. (2012). The island-scale internal
653 wave climate of Moorea, French Polynesia. *Journal of Geophysical Research: Oceans*, 117(6),
654 1-16. doi:10.1029/2012JC007949

655 Lowe, R. J. (2005). Spectral wave dissipation over a barrier reef. *Journal of Geophysical Research*,
656 110(C4), C04001-C04001. doi:10.1029/2004JC002711

657 Lowe, R. J., Falter, J. L., Bandet, M. D., Pawlak, G., Atkinson, M. J., Monismith, S. G., & Koseff, J. R.
658 (2005). Spectral wave dissipation over a barrier reef. *J. Geophys. Res*, 110, 4001-4001.
659 doi:10.1029/2004JC002711

660 Lugo-Fernández, A., Roberts, H. H., & Suhayda, J. N. (1998a). Wave transformations across a
661 caribbean fringing-barrier Coral Reef. *Continental Shelf Research*, 18(10), 1099-1124.
662 doi:10.1016/S0278-4343(97)00020-4

663 Lugo-Fernández, A., Roberts, H. H., & Wiseman, W. J. (1998b). Tide effects on wave attenuation and
664 wave set-up on a Caribbean coral reef. *Estuarine, Coastal and Shelf Science*, 47(4), 385-393.
665 doi:10.1006/ecss.1998.0365

666 Mandlier, P. G. (2013). Field observations of wave refraction and propagation pathways on coral reef
667 platforms. *Earth Surface Processes and Landforms*, 38(9), 913-925. doi:10.1002/esp.3328

668 Masselink, G., Beetham, E., & Kench, P. (2020). Coral reef islands can accrete vertically in response to
669 sea level rise. *Sci. Adv*, 6(June), 3656-3666. Retrieved from <http://advances.sciencemag.org/>

670 Monismith, S. G., Herdman, L. M. M., Ahmerkamp, S., & Hench, J. L. (2013). Wave Transformation
671 and Wave-Driven Flow across a Steep Coral Reef. *Journal of Physical Oceanography*, 43(7),
672 1356-1379. doi:10.1175/jpo-d-12-0164.1

673 Monismith, S. G., Rogers, J. S., Kowek, D., & Dunbar, R. B. (2015). Frictional wave dissipation on a
674 remarkably rough reef. *Geophysical Research Letters*, 42(10), 4063-4071.
675 doi:10.1002/2015GL063804

676 Munk, W. H., & Sargent, M. C. (1948). Adjustment of Bikini Atoll to ocean waves. *Transactions*,
677 *American Geophysical Union*, 29(6), 855-855. doi:10.1029/TR029i006p00855

678 Nielsen, P., Guard, P. A., Callaghan, D. P., & Baldock, T. E. (2008). Observations of wave pump
679 efficiency. *Coastal Engineering*, 55(1), 69-72.
680 doi:<http://dx.doi.org/10.1016/j.coastaleng.2007.07.003>

681 Pequignet, A.-C., Becker, J. M., Merrifield, M. A., & Boc, S. J. (2011). The dissipation of wind wave
682 energy across a fringing reef at Ipan, Guam. *Coral Reefs*, 30, 71-82.

683 Péquignet, A. C., Becker, J. M., Merrifield, M. A., & Boc, S. J. (2011). The dissipation of wind wave
684 energy across a fringing reef at Ipan, Guam. *Coral Reefs*, 30(SUPPL. 1), 71-82.
685 doi:10.1007/s00338-011-0719-5

686 Pomeroy, A., Lowe, R., Symonds, G., Van Dongeren, A., & Moore, C. (2012). The dynamics of
687 infragravity wave transformation over a fringing reef. *Journal of Geophysical Research:*
688 *Oceans*, 117(11). doi:10.1029/2012JC008310

689 Quataert, E., Storlazzi, C., van Rooijen, A., Cheriton, O., & van Dongeren, A. (2015). The influence of
690 coral reefs and climate change on wave-driven flooding of tropical coastlines. *Geophysical*
691 *Research Letters*, 42(15), 6407-6415. doi:10.1002/2015GL064861

692 Roberts, H. H. (1974). *Variability of reefs with regard to changes in wave power around an island*.
693 Paper presented at the Proceedings of the Second International Symposium on Coral Reefs,
694 Brisbane, Brisbane, Australia.

695 Roberts, H. H., Murray, S. P., & Suhayda, J. N. (1975). Physical Processes in Fringing Reef System.
696 *Journal of Marine Research*, 33(2), 233-260. Retrieved from <Go to
697 ISI>://WOS:A1975AL34800006

698 Rogers, J. S., Monismith, S. G., Kowek, D., & Dunbar, R. B. (2016). Wave Dynamics of a Pacific Atoll
699 with High Friction. *Journal of Geophysical Research - Oceans*, 120, 1-18.

700 Samosorn, B., & Woodroffe, C. D. (2008). Nearshore wave environments around a sandy cay on a
701 platform reef, Torres Strait, Australia. *Continental Shelf Research*, 28(16), 2257-2274.
702 doi:10.1016/j.csr.2008.03.043

703 Shannon, A. M., Power, H. E., Webster, J. M., & Vila-Concejo, A. (2013). Evolution of coral rubble
704 deposits on a reef platform as detected by remote sensing. *Remote Sensing*, 5(1), 1-18.
705 doi:10.3390/rs5010001

706 Storlazzi, C. D., Brown, E. K., Field, M. E., Rodgers, K., & Jokiel, P. L. (2005). A model for wave control
707 on coral breakage and species distribution in the Hawaiian Islands. *Coral Reefs*, 24(1), 43-55.
708 doi:10.1007/s00338-004-0430-x

709 Storlazzi, C. D., Elias, E., Field, M. E., & Presto, M. K. (2011). Numerical modeling of the impact of sea-
710 level rise on fringing coral reef hydrodynamics and sediment transport. *Coral Reefs*,
711 30(SUPPL. 1), 83-96. doi:10.1007/s00338-011-0723-9

712 Storlazzi, C. D., Elias, E. P. L., & Berkowitz, P. (2015). Many Atolls May be Uninhabitable Within
713 Decades Due to Climate Change. *Scientific Reports*, 5(1), 1-9. doi:10.1038/srep14546

714 Storlazzi, C. D., Logan, J. B., & Field, M. E. (2003). Quantitative morphology of a fringing reef tract
715 from high-resolution laser bathymetry: Southern Molokai, Hawaii. *Geological Society of
716 America Bulletin*, 115(11), 1344-1355. doi:10.1130/b25200.1

717 Storlazzi, C. D., Ogston, A. S., Bothner, M. H., Field, M. E., & Presto, M. K. (2004). Wave-and tidally-
718 driven flow and sediment flux across a fringing coral reef: Southern Molokai, Hawaii.
719 *Continental Shelf Research*, 24, 1397-1419. doi:10.1016/j.csr.2004.02.010

720 Temmerman, S., Meire, P., Bouma, T. J., Herman, P. M. J., Ysebaert, T., & De Vriend, H. J. (2013).
721 Ecosystem-based coastal defence in the face of global change. In (Vol. 504, pp. 79-83).

722 Tolman, H. L. (2009). *User manual and system documentation of WAVEWATCH III version 3.14*.
723 Retrieved from https://polar.ncep.noaa.gov/mmab/papers/tn276/MMAB_276.pdf

724 Trapon, M. L., Pratchett, M. S., & Penin, L. (2011). Comparative Effects of Different Disturbances in
725 Coral Reef Habitats in Moorea, French Polynesia. *Journal of Marine Biology*, 2011, 1-11.
726 doi:10.1155/2011/807625

727 Van Zanten, B. T., Van Beukering, P. J. H., & Wagtendonk, A. J. (2014). Coastal protection by coral
728 reefs: A framework for spatial assessment and economic valuation. *Ocean and Coastal
729 Management*, 96, 94-103. doi:10.1016/j.ocecoaman.2014.05.001

730 Vetter, O., Becker, J. M., Merrifield, M. A., Pequignet, A. C., Aucan, J., Boc, S. J., & Pollock, C. E.
731 (2010). Wave setup over a Pacific Island fringing reef. *Journal of Geophysical Research-
732 Oceans*, 115, 1-13. doi:10.1029/2010jc006455

733 Vila-Concejo, A., Duce, S., Nagao, M., Nakashima, Y., Ito, M., Fujita, K., & Kan, H. (2017). Typhoon
734 Waves on Coral Reefs. *Coastal Dynamics 2017*(263), 697-701.

735 Vila-Concejo, A., Harris, D. L., Power, H. E., Shannon, A. M., & Webster, J. M. (2014). Sediment
736 transport and mixing depth on a coral reef sand apron. *Geomorphology*, 222, 143-150.
737 doi:10.1016/j.geomorph.2013.09.034

738 Washburn, L. (2015). *MCR LTER: Coral Reef Ocean Currents and Biogeochemistry: salinity,
739 temperature and current at CTD and ADCP mooring FOR01 from 2004 ongoing*.

740 Washburn, L., & Brooks, A. J. (2016). *MCR LTER: Coral Reef: Gump Station Meteorological Data,
741 ongoing since 2006. knb-lter-mcr.9.41*

742 Woodhead, A. J., Hicks, C. C., Norström, A. V., Williams, G. J., & Graham, N. A. J. (2019). Coral reef
743 ecosystem services in the Anthropocene. *Functional Ecology*, 33(6), 1023-1034.
744 doi:10.1111/1365-2435.13331
745 Woolsey, E., Bainbridge, S. J., Kingsford, M. J., & Byrne, M. (2012). Impacts of cyclone Hamish at One
746 Tree Reef: Integrating environmental and benthic habitat data. *Marine Biology*, 159(4), 793-
747 803. doi:10.1007/s00227-011-1855-8
748